

# Spatial Evolution of Plasma Waves in the Acceleration Region and Near-field of a Magnetically Shielded Hall Thruster

Zachariah A. Brown\* and Benjamin A. Jorns†  
University of Michigan, Ann Arbor, Michigan, 48105

The development and propagation of the electron cyclotron drift instability are experimentally characterized in the acceleration region and near field plume of a 9kW magnetically shielded Hall thruster. High speed measurements of ion saturation current are related to plasma density oscillations in the thruster and analyzed to create spatially resolved dispersion relations. Along channel centerline, and between the exit plane of the thruster and 2.5 cm downstream, spectral power is primarily concentrated at distinct bands in the 3-20 MHz domain, indicative of electron cyclotron resonance peaks. Beyond 2.5 cm a linear ion-acoustic like dispersion is seen up to at least 12 cm downstream. The linear wave is dominant in the  $E \times B$  direction at frequencies ranging from 70-300 kHz, wavelengths between 12-53 mm, and with a phase speed of 3700 m/s. Spatially resolved power spectra show a correlation between the emergence of the linear wave and changes in wave energy at high frequencies as the instability propagates downstream from the acceleration region.

## I. Nomenclature

$k$	=	Dispersion wavenumber
$k_x$	=	Axial wavenumber
$k_y$	=	Azimuthal wavenumber
$k_z$	=	Radial wavenumber
$\lambda_D$	=	Debye length
$\rho$	=	Larmor radius
$\phi$	=	Plasma potential
$T_e$	=	Electron temperature
$V_d$	=	Azimuthal electron drift velocity
$V_p$	=	Ion beam velocity
$V_{the}$	=	Electron thermal speed
$\omega$	=	Dispersion frequency
$\omega_{ce}$	=	Electron cyclotron frequency
$\omega_{pi}$	=	Ion plasma frequency

## II. Introduction

ALL thrusters are a form of electric propulsion employing crossed electric and magnetic fields to produce thrust. These devices have an annular, axisymmetric geometry where a strong radial magnetic field confines the electrons in an azimuthal  $E \times B$  current that serves as an efficient ionization source while an electric field accelerates ions across magnetic field lines to produce thrust. Originally conceived in the 1960s, these thrusters are commonly used in satellite station keeping [1] and are being considered for higher power missions such as propulsion for crewed Mars transports [2]. Although moderate power systems are considered a mature technology, as the required lifetime (50,000 hours in some cases) and power requirements of these systems increase, it is becoming increasingly challenging to design and qualify these thrusters using vacuum facility tests. Besides the practical issues of operating a thruster continuously in a vacuum facility for years, there would still be doubt about differences between operation in a vacuum chamber and on orbit. In ground testing facilities, the conductive walls provide a current path not available in space and there

\*PhD Candidate, Department of Aerospace Engineering, brownzac@umich.edu, AIAA Student Member

†Assistant Professor, Department of Aerospace Engineering, bjorns@umich.edu, AIAA Senior Member.

is a limit to how low pressures can be made. These issues give rise to a need for theoretical models and simulations that can quickly validate Hall thruster lifetimes and reliably predict performance. While progress has been made in modeling Hall thrusters, and codes are used in current mission planning [2], there still is no self-consistent model of a Hall thruster. This is because there are key aspects of Hall thruster operation that are not understood, in particular the process governing the motion of electrons across magnetic field lines.

Classically, electrons only travel across magnetic field lines due to particle collisions, but the measured electron mobility in Hall thrusters is orders of magnitude greater than can be explained by collisions. This is the so-called problem of anomalous electron transport. Given the importance of understanding this process for modeling, there have been a myriad of both analytical and experimental attempts to understand this process. Potential models have revolved around wall-effects[3, 4], Bohm diffusion, and micro/macro-turbulence[5–7]. Most recently, a leading theory has emerged, first proposed by Adam et al. [7] based on fully kinetic 2D simulations, that the electron cyclotron drift instability (ECDI) is the primary cause of anomalous transport. Numerous numerical and analytical works have followed to further support the idea of ECDI driven transport in Hall thrusters [8–13].

In addition to the large body of theoretical work supporting the role of the ECDI, the instability was experimentally detected in a Hall thruster plume using collective light scattering techniques [14, 15]. Here, plasma oscillations were recorded as being turbulent and with linear dispersion similar to an ion-acoustic wave. This measured dispersion was predicted by analytical models that assume the ECDI propagates slightly along magnetic field lines[9]; a result also recorded by light scattering measurements. However, in the measured wavenumber domain (5000-12000 rad/m), the amplitude of density fluctuations was smaller than expected by theory, and no local power spectrum peak was detected. In fact, power was seen to monotonically decrease with increasing wavenumber and frequency. Simulation results predicted that the waves should be concentrated at cyclotron resonances that were within the measurable domain of the light scattering experiment[8]. This implies that although the ECDI was experimentally detected, its dispersion was not necessarily consistent with the working theoretical model. In particular, the power spectrum had the wrong shape and amplitude, and using quasilinear theory the wave was too weak to explain explain cross-field transport.

One of the most pressing open questions concerned where most of the energy in the spectrum is concentrated. We recently used direct probe measurements of a Hall thruster plume to find turbulent waves bearing strong resemblance to the ECDI seen by light scattering, but with dominant wavenumbers and frequencies around 120 rad/m and 100 kHz respectively[16]. Applying quasi-linear theory it was shown that the detected turbulence could be responsible for anomalous transport of electrons in the near-field plume. This confirmed the initial assessments from the light scattering experiment: the wave energy was focused at wavenumbers much smaller than predicted, but once accounted for, the ECDI could explain the local cross-field transport. Despite these promising results there remain several questions regarding the nature of the ECDI in Hall thrusters and its impact on electron transport. In particular it is still unclear where in the channel these waves form and how they spatially evolve. It is possible that the downstream spectrum is where the individual resonances have smoothed into a linear dispersion, but that near the acceleration region where the wave is thought to originate the resonances are still prominent. In light of these questions, the need is apparent to measure the dispersion of oscillations in the thruster's acceleration region and track how it evolves in form and power as it travels downstream.

The goal of this investigation is to address this outstanding need by characterizing experimentally the growth and propagation of plasma turbulence in the acceleration region and the near-field plume. The article is organized in the following manner. In Section III, current models of the electron cyclotron drift instability are reviewed and compared to existing experimental data. In Section IV we describe the setup and methodology employed to measure and analyze plasma waves and in Section V the results are presented. Finally in Section VI we compare the results to current theory and draw conclusions about the nature of the ECDI in Hall thrusters.

### III. Review of Electron Cyclotron Drift Instability

Hall thrusters are known to host a myriad of different instabilities due to wide range of energy sources such as high drift velocities, temperature gradients, density gradients, etc [17]. The ECDI is a type of kinetic drift-driven wave in a partially magnetized plasma. The high electron drift velocity at the acceleration region of Hall thrusters can give rise to this instability with the wave growing at the expense of electron kinetic energy through inverse cyclotron resonance. The ECDI in Hall thrusters was first predicted by the fully kinetic 2D simulations of Adam et al. in 2004 [7]. The simulation and following analysis [13] were remarkable due to the ability to resolve many important Hall thruster behaviors, such as the breathing mode oscillation and enhanced mobility without the use of any adjustable parameter. Simulations showed the formation of an instability with small wavelength, on the order of the electron Larmor radius,

and frequencies between 1 and 10 MHz. The key high features of this instability were that it oscillated at discrete wavenumber resonances, propagated in the  $E \times B$  direction, and was strong enough to be drive anomalous transport.

A model of the dispersion relation was later derived [8] that showed, when considering a 2D wave only propagating perpendicularly to magnetic field lines, the instability should be peaked at multiples of the electron Larmor radius. The full dispersion relation is given by Eq.1:

$$1 + k^2 \lambda_D^2 + g \left( \frac{\omega - k_y V_d}{\omega_{ce}}, (k_x^2 + k_y^2) \rho^2, k_z^2 \rho^2 \right) - \frac{k^2 \lambda_D^2 \omega_{pi}^2}{(\omega - k_x v_p)} = 0, \quad (1)$$

where  $g(\Omega, X, Y)$  is the Gordeez function defined as

$$g(\Omega, X, Y) = i\Omega \int_0^{+\infty} e^{-X[1-\cos(\varphi)] - \frac{1}{2}\varphi^2 + i\Omega\varphi} d\varphi. \quad (2)$$

Here  $\omega$  is the oscillation frequency,  $\omega_{ce}$  is the electron cyclotron frequency,  $\omega_{pi}$  is the ion plasma frequency,  $k$  is the oscillation wavenumber,  $k_x$  is the wavenumber component traveling in the axial direction,  $k_y$  is the component in the  $E \times B$  direction,  $k_z$  is the component in the radial direction (along magnetic field lines),  $V_d$  is the azimuthal electron drift velocity,  $V_p$  is the ion beam velocity,  $\lambda_D$  is the Debye length, and  $\rho$  is the electron Larmor radius at thermal velocity ( $V_{the} = \sqrt{T_e/M_e}$ ).

To test this theory collective light scattering experiments measured millimeter scale azimuthal plasma oscillations in a Hall thruster plume, but in contrast to simulation, the detected waves revealed no distinct peaks and a monotonic decrease in power with increasing azimuthal wavenumber[14]. In light of this discrepancy the full 3D dispersion relation was studied by Cavalier et al. [9] that showed under certain conditions, such as the wave having finite propagation along magnetic fields, the Larmor resonances smooth to form an ion-acoustic like dispersion, similar to the one measured by light scattering. It has also been showed that this effect could occur when the wave amplitudes become high[18]. The smoothing of the resonances could explain the linear dispersion relation measured by collective light scattering, but the 3D model still predicts a peak in growth rate at a wavenumber on the order of  $1/(2\lambda_D)$ , which was not experimentally observed.

Later time resolved collective scattering measurements on a pulsed magnetron, a crossed-field plasma device similar to a Hall Thruster, also showed an acoustic-like ECDI, but with the high frequency and wavenumber content modulated by a low frequency envelope at approximately 120 kHz[19]. Building on this idea that the ECDI is dominant at lower frequencies and wavenumber, a recent non-linear consideration of the ECDI by Janhunen et al.[20] showed that under typical Hall thruster conditions the ECDI does not transition to an acoustic regime, the cyclotron resonances are visible, and energy is shifted towards small wavenumbers well below the fundamental cyclotron resonance, forming a large wavelength modulated signal. While the non-linear study of the ECDI was only 1D, it is supported by our recent electrostatic probe measurements of ECDI-like plasma oscillations dominant at low wavenumbers [16].

In summary, the ECDI has been proposed to propagate in Hall thruster plumes and be responsible for anomalous transport. The dispersion could take the form of electron cyclotron resonances or a linear dispersion depending how the wave propagates along magnetic field lines, if the wave oscillations are large, or if non-linear effects occur. Experimental evidence points toward a linear ion-acoustic like dispersion, but there is ambiguity about what wavelengths are dominant. Many simulations point toward millimeter scale oscillations, but some preliminary experimental evidence and non-linear theory suggest the wave transitions to oscillations on the order of centimeters. There are also questions about how the wave spatially evolves as it propagates, such as where does the wave saturate and could a non-linear transition be observed experimentally. In the next section we describe an experimental procedure that can generate spatially resolved dispersion relations from the acceleration region to the near field while of tracking changes in spectral power between tens of kilohertz and fifty megahertz.

## IV. Experimental Setup

In this section we give an overview of the thruster and test facility used in this experiment, followed by a review of the measurement and analysis techniques employed.

### A. Thruster

This experimental campaign investigated the H9 magnetically shielded Hall Thruster. The H9 is a new state of the art 9kW laboratory Hall thruster jointly developed by NASA's Jet Propulsion Laboratory, the University of Michigan

and the Air Force Research Laboratory [21]. The H9 employs a specific magnetic field geometry to shield the channel walls from high energy ions and erosion. Magnetically shielded thrusters exhibit other unique characteristics compared to their unshielded counterparts, namely the acceleration region and location of maximum magnetic field strength shifts downstream and some oscillatory behavior is different[22]. For all measurements the H9 was operated at 300 V and 15 A with xenon propellant, 163 sccm anode flow with a 7% cathode flow fraction; the thruster body was electrically tied to the cathode.

## B. Facility

All testing was performed in the Large Vacuum Test Facility (LVTF) at the Plasmadynamics and Electric Propulsion Laboratory (PEPL). The chamber is 9 m long and 6 m in diameter and employed 10 cryopumps to reach a base pressure of  $5 \times 10^{-7}$  Torr-Xe and a working pressure of  $7 \times 10^{-6}$  Torr-Xe. Pressure was recorded using a Stabil Ion gauge located approximated 1 meter downstream of the thruster exit plane. The chamber was equipped with two slow motion stages to adjust the position of thruster relative to probes, and a downstream axial linear motor capable high speed probe injection.

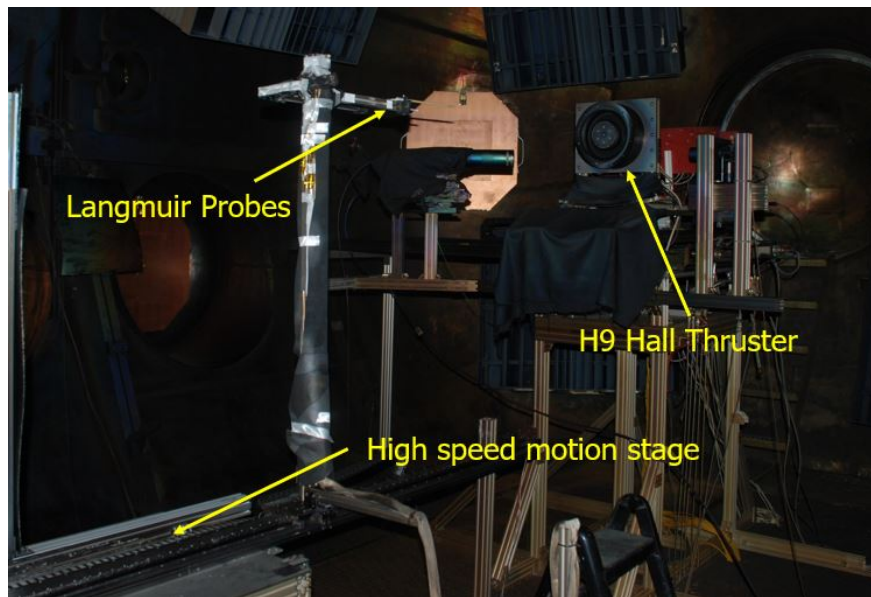


**Fig. 1** Photo of the H9 experimental setup. Diagnostics and motion stages are visible.

## C. Probes

For measurement of plasma waves we used two closely spaced cylindrical Langmuir probes (Fig. 2) set to collect ion saturation current. The probes were set to a bias voltage of -36V relative to facility ground using batteries. Probe tips were made 3.8 mm long and with a radius of 0.38 mm. Smaller probes would increase spatial resolution, but signal to noise would decrease as the probes collect less mean current. The tips were spaced approximately 5 mm apart to allow measurement of wavenumbers up to  $\approx 650$  rad/m. Closer probe spacing increases the maximum measurable wavenumber, but the tips must be kept several Debye lengths apart to ensure their plasma sheaths do not overlap.

We used two different configurations of wave probes in this experiment. We used a quadbore probe (Fig 2a) for measurement of azimuthal and radial wavevectors, where each set of opposing probes measures a single direction. The azimuthal direction ( $k_y$ ) is parallel to the  $E \times B$  direction, the radial direction ( $k_z$ ) is outwards aligned with magnetic field lines, and the axial direction ( $k_x$ ) is parallel to the electric field. To reduce the chance of crosstalk between the probes, voltage was only applied to one set at a time. We measured the axial direction using a single double bore probe (Fig. 2b) with dog-tailed tips to minimize the probe's cross-section in the channel.

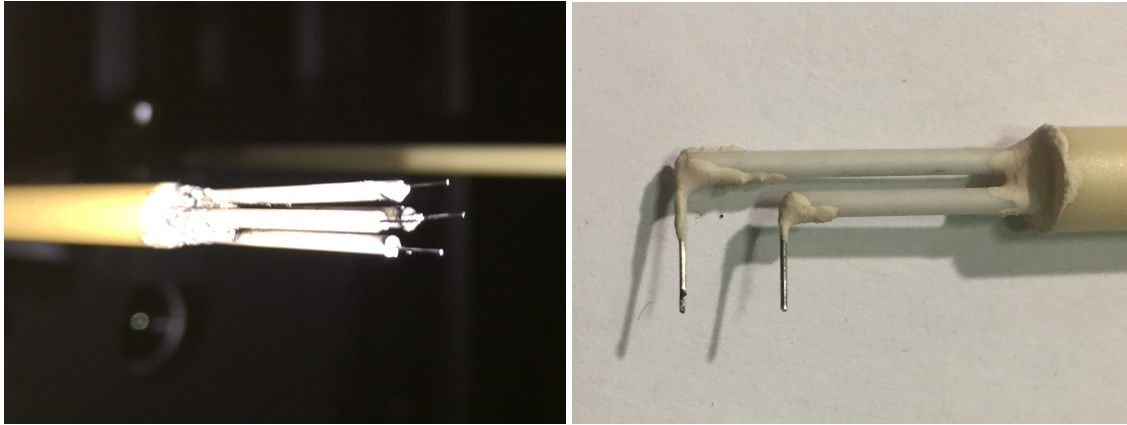
The time-resolved current was inferred by measuring the voltage drop across a 100  $\Omega$  low inductance metal foil resistor with a 16-bit ATS9462 analog waveform digitizer (65 MHz bandwidth). Under the assumption that electron temperature oscillations and wave amplitudes are small, ion saturation current fluctuations can be related to density and

potential oscillations as:

$$\frac{\hat{\phi}}{T_e} = \frac{\hat{n}_i}{\langle n_0 \rangle} = \frac{\hat{i}_{sat}}{\langle i_{sat} \rangle}, \quad (3)$$

where  $\hat{\phi}$  is the local plasma potential perturbation,  $n_0$  is the mean plasma density, and  $i_{sat}$  is ion saturation current;  $\hat{x}$  denotes perturbation values and  $\langle x \rangle$  is a time averaged quantity. Due to the difficulty in measuring plasma parameters in the acceleration region we report potential oscillations relative to electron temperature as volts per electron volt.

Following the methodology of our previous experiments[16, 23], we can generate a statistical representation of the dispersion relation using measurements from the wave probes. Cross-correlation between the time-resolved current collected by each probe yields the phase difference between the two signals, and knowing the probe separation allows calculation of oscillation wavenumber in frequency space. Using the averaged power spectrum and cross-correlation data, intensity plots of oscillations in wavenumber and frequency space are created using the Beall technique[24].



(a) Azimuthal and radial wave probe

(b) Axial wave probe

**Fig. 2** Quadbore wave probe(a): Top and bottom probes tips measure azimuthal waves and left and right tips measure radial waves (b): Axial wave probe

In this campaign we investigated both the near field plume of the thruster and the acceleration region. Signal was recorded continuously at either 10MS/s or 100MS/s as the probe was rapidly injected to and from the exit plane of the thruster with a linear induction motion stage traveling at 50 cm/s. At the exit plane the stage accelerates at 200 cm/s<sup>2</sup> and had a residence time of only 3 ms. Using the known time-dependent trajectory of the motion-stage, time-resolved ion saturation current signals can made be spatial resolved. The waveform is then divided into bins of a fixed spatial width ranging from 1-20 mm (Fig.3). Small position bins give better spatial resolution but at the cost of reduced frequency resolution due to fewer sample points per bin. Beall analysis was performed on each position bin to determine the evolution of plasma waves through the plume and at the acceleration region. While this method is robust and straight forward, it is naturally perturbative and it is possible that the probes are disturbing the local plasma. Yet, so long as we did not probe past the exit plane of the thruster no significant change in discharge current was observed, and currently there is no non-invasive technique capable of yielding similar data for the desired frequencies and wavenumbers.

## V. Results

Here we present the results of Beall analysis along channel center line in the region between the exit plane of the thruster and 12 cm downstream. We start by discussing oscillations in and near the acceleration region and track changes in the spectral content as we look downstream.

### A. Acceleration Region

First we consider the measured dispersion very close to the thruster, between the exit plane and 1 cm downstream. The characteristic Beall intensity plot for this region is shown in Fig. 4. Here the x-axis is wavenumber, the y-axis is frequency, and the color represents the relative intensity of waves at a particular wavenumber and frequency. The Beall plot shows significant dispersion at high frequencies all the way to 50MHz. Using the power spectrum (Fig. 5) we see

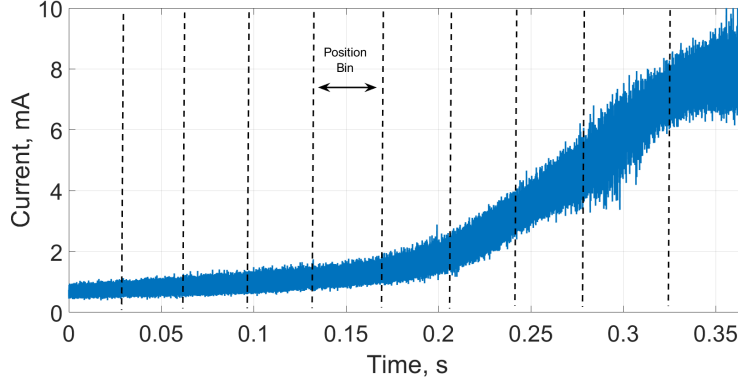


**Fig. 3** Raw waveform shown divided into position bins; bin width not to scale

that the power is concentrated at distinct bands, most noticeably at 3, 5, 8, 15, and 19 MHz, that correspond to the horizontal streak lines in the Beall plot that cut across almost the entire wavenumber domain. Also apparent is the lack of meaningful spectral content around 100-200 kHz or change in the power spectrum across this relatively large spatial domain.

Before moving forward we note that the sharp peak at 1.2 MHz in the power spectrum is assumed to be noise coming from equipment in the facility. It has a wavenumber of zero and its unnormalized amplitude is independent of position in the plume, indicative of pickup in the signal lines from an ambient EM wave.

There are two major conclusions we draw from these findings. First, the ion-acoustic like wave that was previously measured in the near-field plume is not born in the acceleration region. Second, the streak lines seen between 3-20 MHz may be indicative of high wavenumber electron cyclotron resonances from an ECDI that has not yet smoothed into a linear dispersion; we discuss this possibility further in Section VI. In the next section, we explore how the dispersion and power spectrum continue to evolve into the near-field plume.

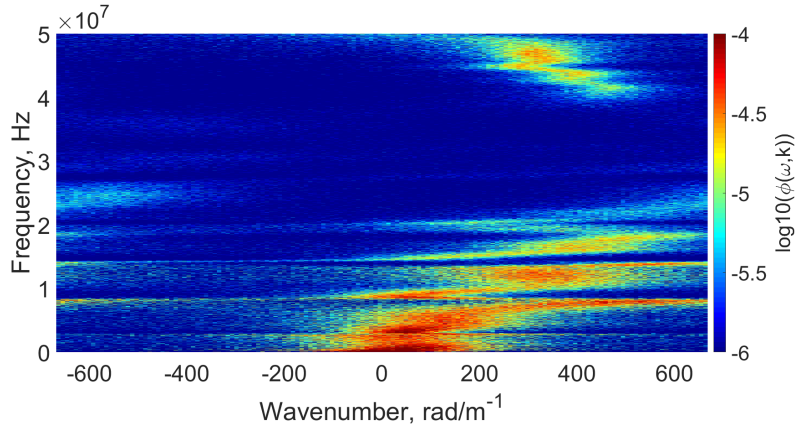


**Fig. 4** Azimuthal Beall intensity plot 1 mm downstream of thruster exit plane

## B. Near-Field

In this section we consider changes in dispersion that occur between 1-12 cm downstream of the exit plane. Using spatial bins 2 cm wide, we see in Fig. 6 that the power spectrum undergoes a drastic change as the wave propagates downstream. The oscillations between 1-20 MHz grow slightly until reaching a maximum approximately 3 cm downstream before decaying down to some equilibrium value around 7 cm. This evolution in high frequency content

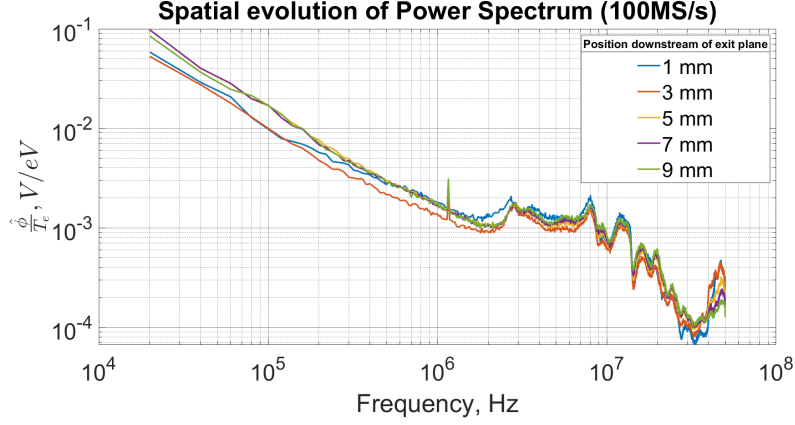


**Fig. 5 Acceleration region: power spectrum vs position downstream of the exit plane**

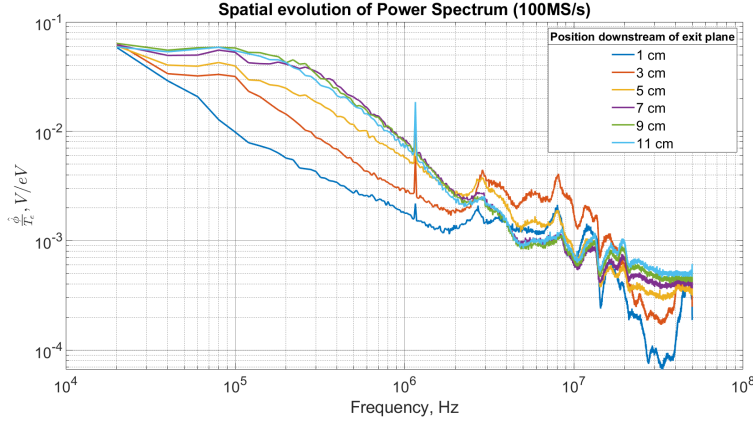


**Fig. 6 Near field: power spectrum vs position downstream of the exit plane**

can be quantified by tracking the normalized wave energy density which we define as:

$$\frac{W}{n_0 T_e} = \sum_{\omega} \left( \frac{\phi(\omega)}{T_e} \right)^2, \quad (4)$$

where the summation of the power spectrum squared is taken over the frequency domain of interest, and again we normalize by local plasma parameters. We see in Fig. 7 that the normalized wave energy in the megahertz domain increases between 1.5 and 3 cm where it peaks before decaying until about 6 cm downstream. Although the magnitude of wave energy remained of the same order implying the wave is saturated.

This peak in high frequency content also corresponds to the emergence of 100-500 kHz spectral content. To investigate this lower frequency content we analyze waveforms collected at a lower sampling rate of 10MS/s. Until about 1.75 cm downstream of the exit plane we only see a streak line near 3 MHz like in the high sampling rate data, but after this location a linear dispersion starts to appear around 100-500 kHz and fully forms by 2.5 cm. See Appendix A for Beall plots as a function of position. Looking at a characteristic Beall plot for the region downstream of 2.5 cm (Fig. 8), we see a linear, ion-acoustic like dispersion in all three wavevectors, but primarily propagating in the azimuthal direction. From the power spectrum (Fig. 8d) we see the turbulence is strongest in the frequency range of 70-300 kHz, corresponding to azimuthal wavenumbers of 90-500 rad/m. Solving for the slope of the azimuthal Beall plot yields a group velocity of 3700 m/s, which is likely on the order of the ion sound speed in the acceleration region and is almost identical to the slope of the dispersion seen by light scattering. Furthermore, with respect to the  $E \times B$  direction, the wave was calculated to propagate at 20 degrees in the axial direction and -3.6 degrees in the radial direction. That is the wave propagates away from the thruster and very slightly opposite the direction of magnetic field lines. This linear

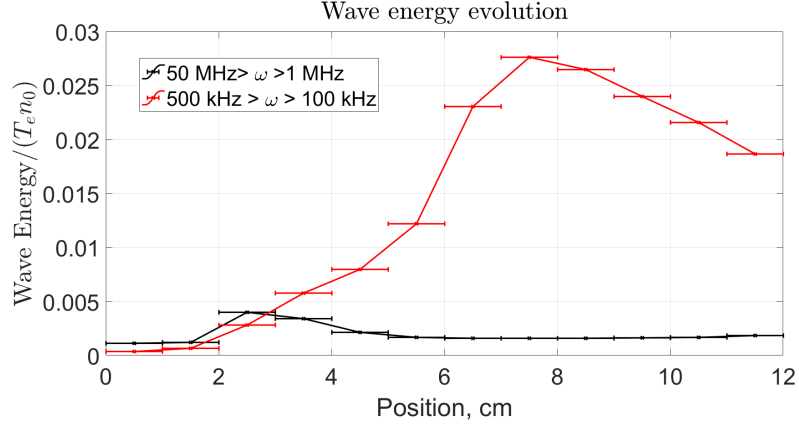


**Fig. 7 Spatial evolution of normalized wave energy at high and low frequencies**

dispersion stays constant in shape at least 12 cm downstream, but we see in the low frequency wave energy (Fig. 7) that the linear turbulence continues to grow until 7 cm downstream, but again changes are within the same order of magnitude.

There are several important conclusions from the data taken in this region. The measured dispersion agrees with the previous near-field wave measurements[16]. The wave direction angles are similar to those inferred from light scattering, -10 degrees in the axial direction and 4.6 degrees in the radial direction[15]. The linear dispersion abruptly appears over a distance of 1 cm, and most interestingly the appearance of this linear wave correlates with changes in the high frequency oscillations.

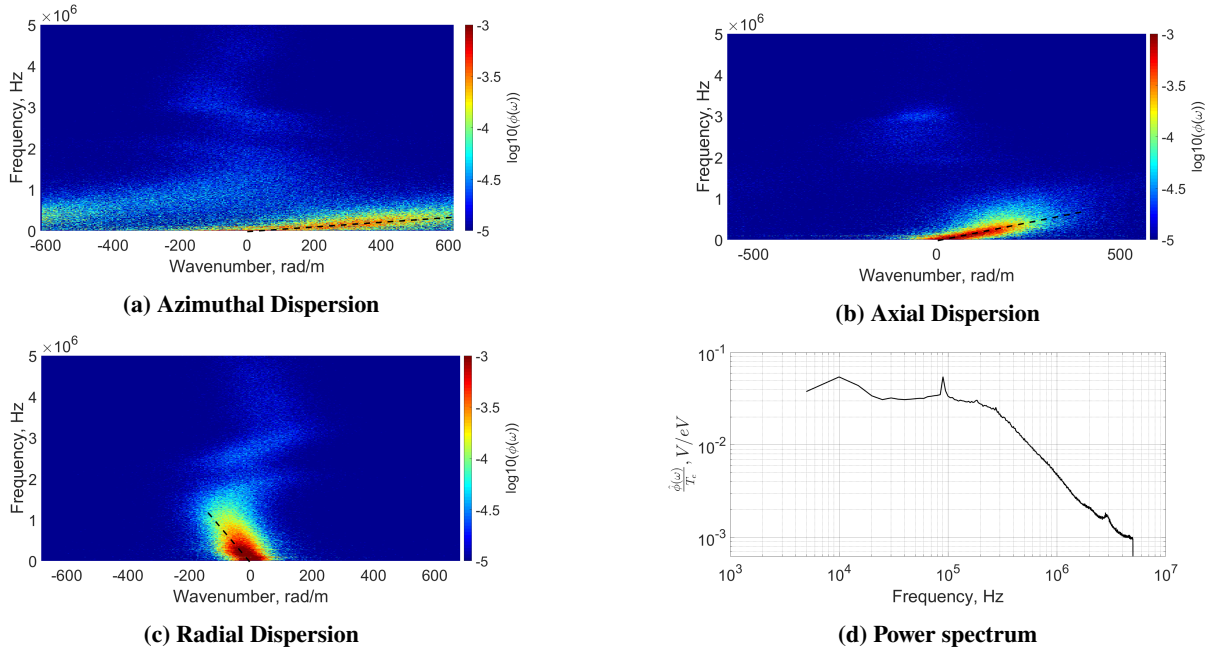
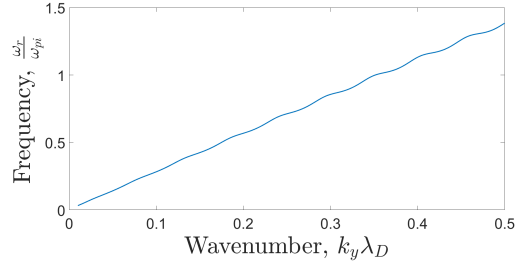


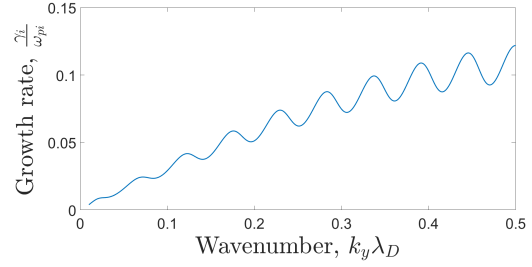
**Fig. 8 Beall intensity plots and power spectrum 4 cm downstream of thruster exit plane**

## VI. Discussion

As previously mentioned, the high frequency streak lines in Fig. 4 could be aliased cyclotron resonance peaks of the ECDI. When this probing technique encounters oscillations with wavenumbers larger than the technique can explicitly



(a) Frequency vs azimuthal wavenumber

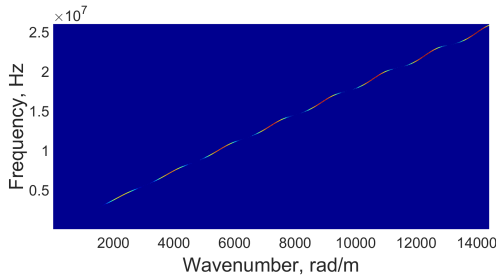


(b) Growth rate vs azimuthal wavenumber

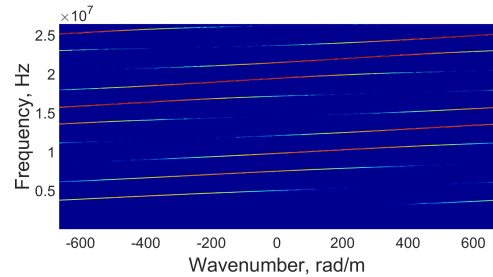
**Fig. 9 Numerical solution to dispersion relation. Frequencies are normalized by ion plasma frequency ( $\omega_{pi}$ ) and wavenumber is normalized by Debye length ( $\lambda_D$ ).**

measure the signal is aliased to a modulus of the maximum measurable wavenumber. For example, a wavenumber of 700 would appear at -50 and a wavenumber of 1400 would appear at 100. This is particularly evident in Fig. 8a where the linear azimuthal dispersion clearly wraps around from 650 to -650 rad/m. For cyclotron resonances with wavenumbers well into the 1000s and 10000s there would certainly be an aliasing effect if detected by our probes. To demonstrate this possibility we numerically solve Eq. 1 using following parameters:  $n_0 = 1.2 \times 10^{18} \text{ m}^{-3}$ ,  $B = 95 \text{ G}$ ,  $T_e = 20 \text{ eV}$ ,  $V_p = 20 \text{ km/s}$ ,  $V_D = V_{the}/2$ ,  $k_z \lambda_D = 0.01$ , and the  $k_x = \tan(20^\circ)k_y$ . These values were chosen to closely approximate the plasma parameters in the acceleration region, and  $k_z$  was made such that the resonances do not smooth out.

The calculated dispersion relation is shown in Fig. 9, where the frequency and growth rate have been normalized by the ion plasma frequency and wavenumber is normalized by the Debye length. We convert this dispersion relation to an artificial Beall plot shown in Fig. 10a where we have taken the intensity as proportional to the growth rate and added Gaussian noise to simulate turbulence. Aliasing this dispersion yields a Beall intensity plot (Fig. 10b) bearing streak lines resembling the measured dispersion in Fig. 4. With the similarities between the numerical and measured Beall plots and the measured frequency bands being close to resonances of each other, we believe it is a reasonable assumption that aliased electron cyclotron resonances were measured.



(a) Unaliased Beall of numerical dispersion relation



(b) Aliased Beall plot intensity of numerical dispersion relation

**Fig. 10 Numerical dispersion relation converted to a Beall intensity plot (a) and into an aliased Beall plot of the measured wavenumber domain (b)**

Following the assumption that we are seeing cyclotron resonances, even far into the near field, a possibility is that ECDI originates in the acceleration region in its non-acoustic form with power at near cyclotron resonances and undergoes an inverse energy cascade, as describe by Janhunen, as it travels downstream. The low wavenumber linear dispersion appears after 2.5 cm downstream, and with an ion beam velocity of 20,000 m/s the characteristic time for this transition is  $1.25 \mu\text{s}$ , which agrees with Janhunen's simulation that the inverse energy cascade occurs on the order of microseconds or slightly faster.

## VII. Conclusions

In this paper we have presented an investigation of plasma waves in the acceleration region and near-field of a magnetically shielded Hall thruster. Spatially resolved dispersion relations implied that ECDI resonances exist in both the acceleration region and near-field plume. Near field plume measurements showed a strong linear dispersion at low frequency and wavenumber that appears after 2.5 cm downstream of the exit plane. Furthermore, we saw that the wave energy density appears to be saturated everywhere in the plume. Finally, we proposed that the linear low frequency oscillations in the near-field developed from the ECDI through non-linear processes.

## VIII. Appendix A: Azimuthal Beam Plots, 1.5-3.5 cm

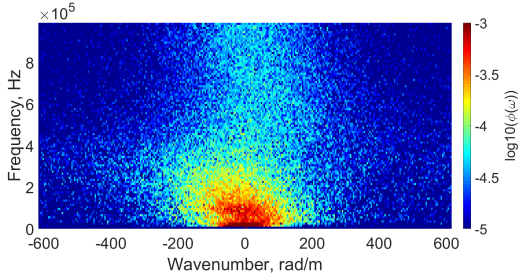


**Fig. 11** Position: 1.5 cm

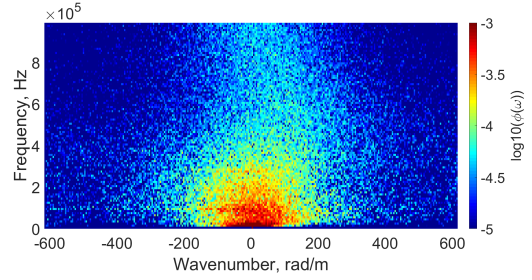


**Fig. 12** Position: 1.75 cm

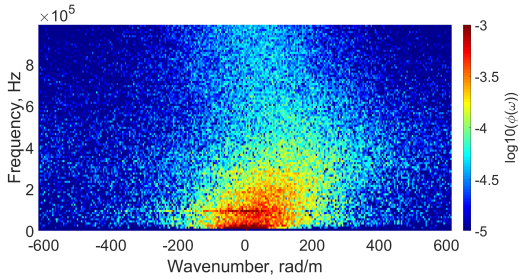


**Fig. 13** Position: 2.0 cm

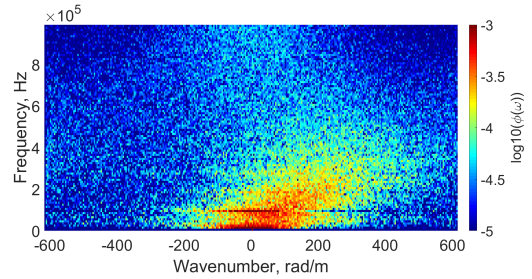


**Fig. 14** Position: 2.25 cm

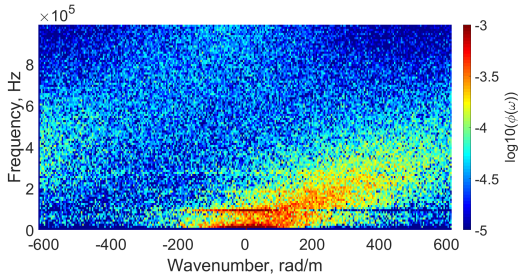


**Fig. 15** Position: 2.5 cm

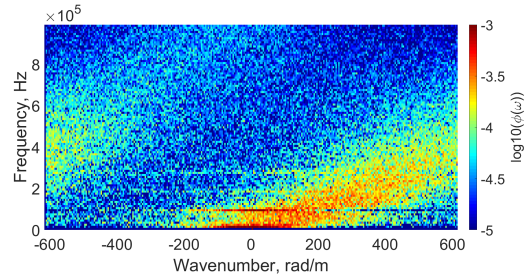


**Fig. 16** Position: 2.75 cm

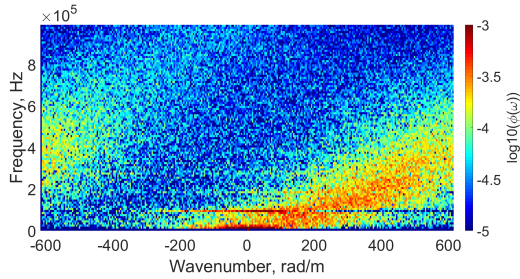


**Fig. 17 Position: 3.0 cm**

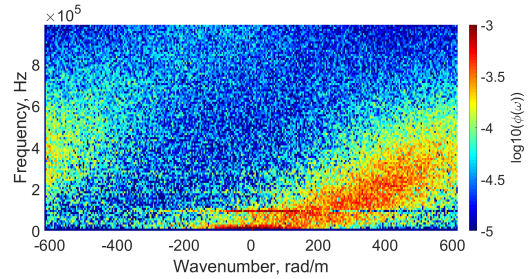


**Fig. 18 Position: 3.5 cm**

## Acknowledgments

Work supported by National Science Foundation Graduate Research Fellowship Program Grant No. DGE s1256260. Any opinions, findings, and conclusions or recommendations expressed in this material are those of the author(s) and do not necessarily reflect the views of the National Science Foundation.

## References

- [1] Martinez-Sanchez, M., and Pollard, J. E., "Spacecraft Electric Propulsion-An Overview," *Journal of Propulsion and Power*, Vol. 14, No. 5, 1986, pp. 688–699.
- [2] Hofer, R., Kamhawi, H., Herman, D., Polk, J., Snyder, J. S., Mikelliedes, I., et al., "Development Approach and Status of the 12.5 kW HERMeS Hall Thruster for the Solar Electric Propulsion Technology Demonstration Mission," *34th International Electric Propulsion Conference*, 2015.
- [3] Barral, S., Makowski, K., Peradzyński, Z., Gascon, N., and Dudeck, M., "Wall material effects in stationary plasma thrusters. II. Near-wall and in-wall conductivity," *Physics of Plasmas*, Vol. 10, No. 10, 2003, p. 4137.
- [4] Gascon, N., Dudeck, M., and Barral, S., "Wall material effects in stationary plasma thrusters. I. Parametric studies of an SPT-100," *Physics of Plasmas*, Vol. 10, No. 10, 2003, p. 4123.
- [5] Thomas, C. A., and Cappelli, M. A., "Gradient transport processes in E x B plasmas," *41st AIAA/ASME/SAE/ASEE Joint Propulsion Conference*, 2005.
- [6] McDonald, M. S., and Gallimore, A. D., "Parametric Investigation of the Rotating Spoke Instability in Hall Thrusters," *32nd International Electric Propulsion Conference*, 2011.
- [7] Adam, J. C., Heron, A., and Laval, G., "Study of stationary plasma thrusters using two-dimensional fully kinetic simulations," *Physics of Plasmas*, Vol. 11, No. 1, 2004, p. 295.
- [8] Ducrocq, A., Adam, J. C., and Heron, A., "High-frequency electron drift instability in the cross-field configuration of Hall thrusters," *Physics of Plasmas*, Vol. 13, No. 10, 2006.
- [9] Cavalier, J., Lemonie, G., N amd Bonhomme, Tsikata, S., Honore, C., and Gresillon, D., "Hall Thruster Plasma Fluctuations Identified as the ExB Electron Drift Instability: Modeling and Fitting on Experimental Data," *Physics of Plasmas*, Vol. 20, 2013, p. 082108.
- [10] Katz, I., Ortega, A. L., Jorns, B. A., and Mikellides, I. G., "Growth and Saturation of Ion Acoustic Waves in Hall Thrusters," *52nd AIAA Joint Propulsion Conference*, 2016.
- [11] Lafleur, T., Baalrud, S. D., and Chabert, P., "Theory for the anomalous electron transport in Hall effect thrusters: I. Insights from particle-in-cell simulations," *Physics of Plasmas*, Vol. 23, 2016, p. 053502.
- [12] Ortega, A. L., Katz, I., and Chaplin, V. H., "A First-Principles Model Based on Saturation of the Electron Cyclotron Drift Instability for Electron Transport in Hydrodynamic Simulations of Hall Thruster Plasmas," *35th International Electric Propulsion Conference*, 2017.
- [13] Adam, J. C., Boeuf, J. P., Dubuit, N., Dudeck, M., Garrigues, L., Gresillon, D., Heron, A., Hagelaar, G. J. M., Kulaev, V., Lemoine, N., Mazouffre, S., Perez Luna, J., Pisarev, V., and Tsikata, S., "Physics, simulation and diagnostics of Hall effect thrusters," *Physics of Plasmas*, Vol. 50, No. 12, 2008, p. 124041.

- [14] Tsikata, S., Lemoine, N., Pisarev, V., and Gresillon, D. M., "Dispersion relation of electron density fluctuations in a Hall thruster plasma, observed by collective light scattering," *Physics of Plasmas*, Vol. 16, No. 3, 2009, p. 033506.
- [15] Tsikata, S., Honore, C., Lemoine, N., and Gresillon, D. M., "Three-dimensional structure of electron density fluctuations in the Hall thruster plasma: E x B mode," *Physics of Plasmas*, Vol. 17, No. 11, 2010, p. 112110.
- [16] Brown, Z. A., and Jorns, B. A., "Dispersion relation measurements of plasma modes in the near-field plume of a 9-kW magnetically shielded thruster," *35th International Electric Propulsion Conference*, 2017.
- [17] Choueiri, E. Y., "Plasma oscillations in Hall thrusters," *Physics of Plasmas*, Vol. 8, 2001, p. 1411.
- [18] Lampe, M., Manheimer, W. M., McBride, J. B., Orens, J. H., Shanny, R., and Sudan, R. N., "Nonlinear Development of the Beam-Cyclotron Instability," *Physics Review Letters*, Vol. 26, No. 20, 1971, p. 1221.
- [19] Tsikata, S., and Minea, T., "Modulated Electron Cyclotron Drift Instability in a High-Power Pulsed Magnetron Discharge," *Physics Review Letters*, Vol. 114, No. 18, 2015, p. 185001.
- [20] Janhunen, S., Smolyakov, A., Chapurin, O., Sydorenko, D., Kaganovich, I., and Raitses, Y., "Nonlinear structures and anomalous transport in partially magnetized ExB plasmas," *Physics of Plasmas*, Vol. 25, No. 1, 2018, p. 011608.
- [21] Hofer, R. R., Cusson, S. E., and Lobbia, R. B., "The H9 Magnetically Shielded Hall Thruster," *35th International Electric Propulsion Conference*, 2017.
- [22] Jorns, B., and Hofer, R., "Plasma oscillations in a 6-kW magnetically shielded Hall thruster," *Physics of Plasmas*, Vol. 21, No. 5, 2014, p. 053512.
- [23] Jorns, B. A., Mikellides, I. G., and Goebel, D. M., "Ion acoustic turbulence in a 100-A LaB<sub>6</sub> hollow cathode," *Phys. Rev. E*, Vol. 90, 2014, p. 063106.
- [24] Beall, J. M., Kim, Y. C., and Powers, E. J., "Estimation of wavenumber and frequency spectra using fixed probe pairs," *Physics of Plasmas*, Vol. 53, 1982, p. 3933.